Solution Studies and Crystal Structures of Heteropolynuclear Potassium/Copper Complexes with Phytate and Aromatic Polyamines:

Solution Study and Crystal Structures of Heteropolynuclear K/Cu Complexes with Phytate and Aromatic Polyamines: Self-Assembly through Coordinative and Supramolecular Interactions

Delfina Quiñone,[a] Sebastián Martínez,[a] Fernando Bozoglián,[b] Carla Bazzicalupi,[c] Julia Torres,[a] Nicolás Veiga,[a] Antonio Bianchi*[c] and Carlos Kremer*[a]

Abstract: Phytate (L^{12-}) is a relevant natural product. It interacts strongly with biologically relevant cations, due to the high negative charge exhibited in a wide pH range. The synthesis and crystal structures of the mixed-ligand Cu(II) polynuclear complexes $K(H_2tptz)_{0.5}[Cu(H_8L)(tptz)]\cdot 3.6H_2O$ (**1**), $K(H_2O)_3\{[Cu(H_2O)(bpca)]_3(H_8L)\}\cdot 1.75H_2O$ (**2**), and $K_{1.5}(H_2O)_2[Cu(bpca)](H_{9.5}L)\cdot 8H_2O$ (**3**) (tptz = 2,4,6-tri(pyridin-2-yl)-1,3,5-triazine; Hbpca = bis(2-pyridylcarbonyl) amine) are reported herein. They were obtained by the use of an aromatic rigid amine, which satisfies some of the metal coordination sites and promotes the hierarchical assembling of 2D polymeric structures. Speciation of phytate-Cu(II)-Hbpca system and determination of complex stability constants were performed by means of potentiometric titrations, in 0.15 M NMe_4Cl at 37.0 °C, showing that, even in solution, this system is able to produce highly aggregated complexes, such as $[Cu_3(bpca)_3(H_7L)]^{2-}$. Furthermore, the Cu(II)-mediated tptz hydrolysis was studied by studied by UV-vis spectroscopy at room temperature in 0.15 M NMe_4Cl. Based on the equlibrium results and with the aid of molecular modelling tools, we were able to propose a plausible self-assembling process for **2** and **3**. All these results give relevant information about the multifaceted coordination ability of phytate and its versatility as building block for the hierarchical assembling of extended structures.

Introduction

myo-Inositol phosphates (Ins*P*s) are a group of important secondary messengers in eukaryotic cells.[1] This family includes a wide variety of metabolically related biomolecules, bearing different phosphorylation patterns over the *myo*-inositol ring. Even though the existence of inositol phosphates in biology has been known for over 80 years,[2] their biological functions are yet to be completely understood.[3]

InsP_6 (L^{12-} representing its fully deprotonated form depicted in Figure 1a), also known as phytate, was the first inositol phosphate discovered,[1] and it is the most abundant member of the family, with intracellular concentrations ranging from 10 μM to 60 μM in animal cells,[4] and up to 700 μM in slime moulds.[5] Given the fact that the eukaryotic organisms have evolved multiple pathways to synthesize it, it is commonly believed that InsP_6 must be somehow important to cell function.[3c] Indeed, phytate has been associated with the regulation of important processes like ion channel and protein trafficking,[6] endocytosis,[7] exocytosis,[8] oocyte maturation,[9] cell division and differentiation,[10] mRNA export,[11] and DNA repair and protein folding.[12] Additionally, multiple pharmacological activities have been ascribed to phytate, related to its antioxidant,[13] antineoplastic[14] and biomineralization[15] properties.

As a highly charged anion, phytate strongly interacts with biologically relevant metal ions, giving rise to an intertwined set of protonation, complexation and precipitation equilibria. Indeed, all mentioned biological activities are related to its intricate coordination chemistry.[16] The lack of knowledge about the chemical and structural features of the InsP_6-M^{n+} species has been the main setback to the experimental research on its biological roles and pharmacological activities.[16b] In this context, our group has devoted several years to study the stability[17] and structural features[18] of in-solution phytate-metal species. Nevertheless, due to the amorphous characteristic of the InsP_6-M^{n+} complexes in the solid state, an in-depth X-ray structural analysis of the phytate multifaceted coordination ability is not

[a] D. Quiñone, Dr. S. Martínez, Prof. J. Torres, Prof. N. Veiga, Prof. C. Kremer
Facultad de Química
Universidad de la República
Uruguay
E-mail: ckremer@fq.edu.uy
[b] Dr. F. Bozoglián
Institut Català d'Investigació Química
Tarragona
Spain
[d] Prof. C. Bazzicalupi, Prof. A. Bianchi
Department of Chemistry "Ugo Schiff"
University of Florence
Sesto Fiorentino
Italy
E-mail: Antonio.bianchi@unifi.it

Supporting information for this article is given via a link at the end of the document.

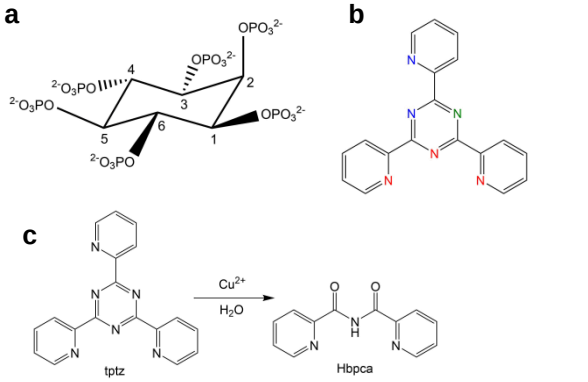

Figure 1. Structure of phytate anion (a) and 2,4,6-tri(pyridin-2-yl)-1,3,5-triazine (tptz) (b). In aqueous media, Cu(II) ions promote the hydrolysis of tptz to form bis(2-pyridylcarbonyl) amine (Hbpca) (c).

straightforward. The structure of $Na_{12}L{\cdot}38H_2O$, reported in 1975,[19] had remained for many years the unique solved crystal structure of a compound containing a metal ion and InsP_6. Very recently, the structures of $[Zn_{10}(H_2L)_2]{\cdot}xH_2O$[20] and $K_3(H_9L){\cdot}2H_2O$[21] have been reported.

We previously reported four crystalline structures of phytate-metal complexes determined by X-ray diffraction (XRD): $(H_2terpy)_2[Mn(H_6L)(terpy)(H_2O)]{\cdot}17H_2O$, $K[Cu_4(H_3L)(terpy)_4]{\cdot}26H_2O$, $[Cu_5(H_7L)_2(H_2O)_2(phen)_5]{\cdot}23H_2O$ and $[Cu_2(H_8L)(terpy)_2]{\cdot}7{,}5H_2O$ (terpy = 2,2':6',2"-terpyridine; phen = 1,10-phenanthroline).[22] These compounds were obtained by the use of an aromatic rigid polyamine, which acts as an auxiliary ligand, satisfying some of the metal coordination sites and facilitating crystallization. The polyamine also emulates the presence of other chelating ligands sharing the biological compartments, allowing gathering relevant structural information about the multifaceted coordination ability of phytate under simulated physiological conditions.

In the quest for new coligands to test, we included in our studies a bulky heterocyclic compound named 2,4,6-tris(2-pyridyl)-*s*-triazine (tptz, the neutral form also designed tptz, depicted in Figure 1b), featuring three 2-pyridyl rings and a 1,3,5 triazine ring.[23] This commercially available ligand is particularly suitable for our goals on several grounds. First, it bears a large delocalized π system that can facilitate packing and crystallization. Besides, it shows a versatile coordination chemistry, with different coordination modes and denticities, which has been studied for more than 50 years.[24] Frequently, tptz forms mononuclear complexes through its terpyridine-like tridentate coordination site, while the use of the other two coordination sites are less common due to metal-mediated inductive effects.[25] In this framework, it is not surprising that tptz has drawn much attention since it was first synthesized.[23] Its metal complexes have found application in the spectroscopic determination of metal ions and molecules,[26] the separation of lanthanides and actinides ions,[27] the preparation of DNA cleavage agents,[28] luminescent sensing[29] and catalysis.[30]

On consideration of the multiple binding properties of phytate and tptz, we thought that their involvement in a three-component system, including a metal ion, would be able to furnish the basis for the self-assembling of new extended structures. For this reason, we investigated the phytate/tptz/Cu(II) system, succeeding in the preparation of new materials in which the hierarchical action of coordination and supramolecular forces directed the formation of 2D structures, where phytate is responsible for the formation of 1D polymeric coordination chains that are turned into the 2D assemblies through the supramolecular interactions established by auxiliary ligand molecules. During this study, we observed that, in aqueous media, the phytate/tptz/Cu(II) system gave readily rise to compounds containing the hydrolytic derivative of tptz bis(2-pyridylcarbonyl) amine (represented in general as Hbpca, also designing the neutral form shown in Figure 1c). For these compounds, Hpbca was found to direct the construction of a 2D supramolecular assembly.

The hydrolysis of tptz in the presence of Cu(II) was first found by Lerner and Lippard,[31] and since it was reported later for other metal cations,[32] it has been ascribed to a metal-mediated electron-withdrawing effect. The *in situ* generation of Hbpca increases the ligand's structural versatility, giving rise to a new family of metal complexes with attractive magnetic and supramolecular properties.[33] The nature of the isolated hydrolytic products seems to be strongly dependent on the nature of the anion present in solution.[34] Although the influence of mono- and dicharged anions was reported,[34-35] highly charged anions such as phytate have never been tested.

From this perspective, we present here the synthesis and characterization of three novel Cu(II)-phytate complexes containing tptz or bpca$^-$: $K(H_2tptz)_{0.5}[Cu(H_8L)(tptz)]{\cdot}3.6H_2O$ (**1**), $K(H_2O)_3\{[Cu(H_2O)(bpca)]_3(H_8L)\}{\cdot}1.75H_2O$ (**2**), and $K_{1.5}(H_2O)_2[Cu(bpca)](H_{9.5}L){\cdot}8H_2O$ (**3**). Their structures were solved by XRD and discussed comparatively in the light of other tptz, Hbpca and phytate metal complexes reported so far. Beside the formation of the self-assembled coordination/supramolecular 2D structures, which involves an ubiquitous natural product, we performed the speciation of the phytate/Hbpca/Cu(II) ternary system in aqueous solution. This was also taken as a reference model for the self-assemblies arising from the phytate/tptz/Cu(II) system, on account of the instability of tptz in water. The study was complemented with the analysis of the spectroscopic features of the new compounds and of the hydrolytic properties of the Cu/tptz system, helped by molecular modelling that also gave support to the formulation of the proposed self-assembling process of the new extended structures.

Results and Discussion

Crystal structure description

The crystal structure of **1** consists of 1D $\{K[Cu(tptz)(H_8L)]\}_n^{n-}$ polymeric coordination chains growing along the *c* crystallographic axis, intercalated with $(H_2tptz)^{2+}$ cations and co-crystallized with water molecules. Each phytate H_8L^{4-} anion is in the 1 axial-5 equatorial (1a5e) *myo*-inositol conformation, with only one phosphate group in axial position (P2), and involves all its phosphate groups, but one, in connecting three symmetry related potassium cations (Figure 2). Couples of adjacent phosphate groups (P1-P6, P2-P3, P3-P4) bind the same K^+ ion

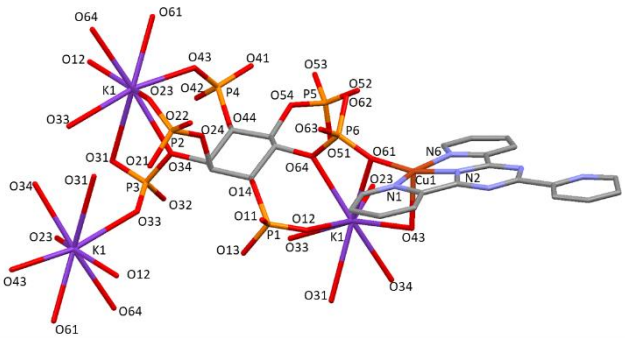

Figure 2. The basic structural unit in **1** with labelling scheme (H atoms omitted). Color code: C, grey, O, red, N, light blue, P, orange, K, violet, Cu, brown.

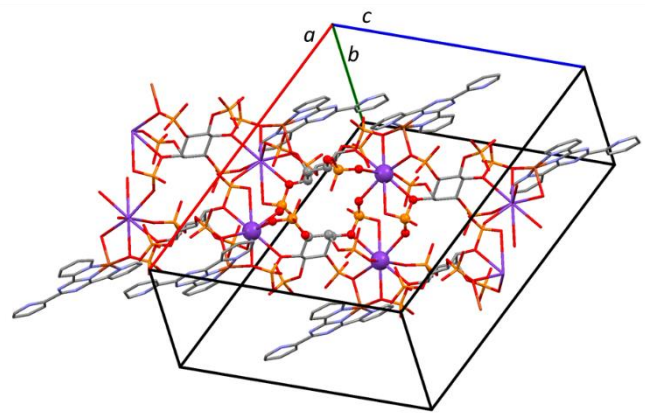

Figure 3. 1D $\{K[Cu(tptz)(H_8L)]\}_n^{n-}$ polymeric coordination chain in **1** growing along the c crystallographic axis. Ball and stick graph is used to evidence the 20-membered and the 8-membered rings (H atoms omitted).

forming 7-membered chelate rings, while phosphates P1 and P3 bind two metal centres through a nine-atom arch. The phosphoester oxygen atoms of the phosphate groups P3 and P6 complete the 8-coordination environment of the K^+ ion.

The $\{K[Cu(tptz)(H_8L)]\}^-$ unit is replicated along the *c* crystallographic axis, giving rise to the 1D polymeric structure, whose skeleton is formed by $(H_8L)^{4-}$ and K^+ ions, containing 20-membered rings (each around a 2-fold axis) and 8-membered rings (each around an inversion centre), alternating along the chain (Figure 3). The 20-membered rings are generated by two of the above-described nine-atom arches bridging the same pair of K^+ ions. These polymeric coordination chains are decorated with $[Cu(tptz)]^{2+}$ groups, which are held in place by coordination to Cu(II) of the oxygen atoms O43 and O61 from P4 and P6 phosphate groups of different phytate anions. The Cu(II) ion is penta-coordinated in a slightly distorted square pyramidal environment with O43 in apical position. Each coordinated tptz molecule interacts via π-stacking with a not-coordinated $(H_2tptz)^{2+}$ cation, which acts as the glue that sticks together two adjacent 1D chains (mean π-π interplanar distances of 3.5 Å), generating a 2D supramolecular assembly. The location of coordinated tptz molecules and not-coordinated $(H_2tptz)^{2+}$ cations with respect to the 1D polymeric chains is shown in Figures 4 and S1. An H-bond network formed by the co-crystallized water molecules contributes to stabilize the crystal packing. Nevertheless, these water molecules are mainly disordered, so their contacts are not further discussed.

As already observed in the previous structure, also (**2**) contains phytate anions in 1a5e conformation. One phosphate group is disordered: it adopts two conformations with similar coordination behaviour. Accordingly, only one of them is discussed here. All phosphate groups of the $(H_8L)^{4-}$ phytate anion are involved in metal coordination. As shown in Figure 5, each of the three P1, P3 and P4 groups is involved in the coordination of a copper ion, whose square pyramidal coordination sphere is completed by the three nitrogen atoms of a $bpca^-$ anion and a water molecule placed in the apical position. The P2, P5 and P6 phosphates participate to the coordination of symmetry related potassium ions. Each K^+ is actually heptacoordinated by three phosphate oxygens, three water

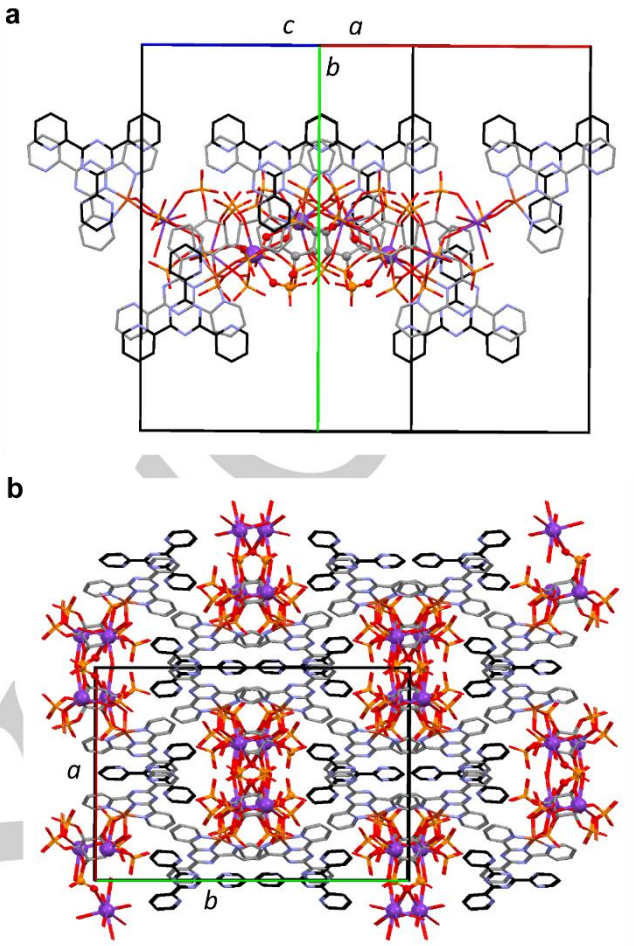

Figure 4. a) Relative locations of coordinated tptz molecules and not-coordinated $(H_2tptz)^{2+}$ cations with respect to the 1D-polymeric chain in **1**, generating the 2D supramolecular assembly. b) Crystal packing viewed along the c axis. H atoms and co-crystallized water molecules were omitted. Not coordinated $(H_2tptz)^{2+}$ cations are coloured in black.

molecules and the carbonyl oxygen (O3) from one of the three $bpca^-$ anions present in the asymmetric unit. Two copper ions (Cu2, Cu3) and the potassium ion are bridged by the phytate units giving rise to 1D polymeric coordination chains of $(K(H_2O)_3\{[Cu(H_2O)(bpca)]_3H_8L\})_n$ formula, which grow along the *b* crystallographic axis (Figure 6). Centrosymmetric 32-membered and 24-membered rings are formed, which alternate along the chain. As shown in Figure 6, the $[Cu_2(bpca)]$ units only belong to the 32-membered ring, while Cu3 contributes to define both the 32- and 24-membered ones. The $bpca^-$ ligand coordinated to Cu3 resides inside the larger ring, where π-stacking interactions are established between the four $bpca^-$ anions bound to the Cu2 and the Cu3 metal centres in the ring (interplanar distances about 3.2 Å). Conversely, the Cu1 copper ions and their coordinated $bpca^-$ ligands are facing outwards and provide the connection with other parallel chains via π-π stacking interactions with the $[Cu_2(bpca)]$ units (Figure 7), giving rise to a 2D supramolecular assembly. It is worth noting that two symmetry related water molecules are inserted into the 32-membered ring, forming H-bond contacts with the O51 phytate oxygen (O51···OW2, 3.25(1) Å) and the O6 carbonyl oxygen

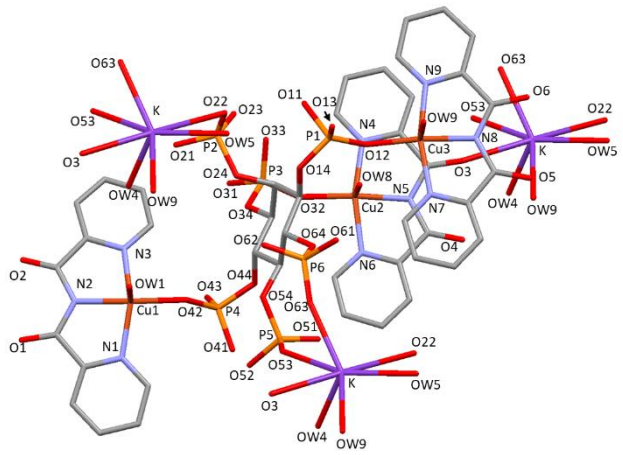

Figure 5. The basic structural unit in **2** with labelling scheme (H atoms omitted). Color code: C, grey, O, red, N, light blue, P, orange, K, violet, Cu, brown.

from the Cu_3L_2 assembly (O6···OW2, 2.67(1) Å). This water molecule is well placed to give a lone pair-π interaction with one of the pyrimidine ring of the $[Cu_2(bpca)]$ assembly (Figure S2; OW2···pyridine plane, OW2··· pyridine centroid, offset distances: 3.14, 3.16 and 0.35 Å, respectively). The remaining water molecules coordinated to the metal centres form H-bond contact with carbonyl oxygens of $bpca^-$ and with phosphate oxygens of the phytate anions.

The structure of **3** shows remarkable analogies with the $K(H_2tptz)_{0.5}[Cu(tptz)(H_8L)]\cdot 3.6H_2O$ compound. Indeed, as shown in Figures 8 and 9, in the 1D polymeric coordination chain of $\{K_{1.5}(H_2O)_2[Cu(bpca)](H_{9.5}L)\}_n$ formula, phytate (1a5e conformation) and K^+ ions form the skeleton of the chain, phytate bridges three symmetry related K1 ions and forms 20-membered and 8-membered rings. Also, in this case one phosphate group is spread over two positions showing similar coordination behaviours. Accordingly, only one of them will be discussed here. All phosphate groups but P5 are involved in metal coordination, forming the P1-P6, P2-P3 and P3-P4 7-membered chelate rings, as well as the nine-atom arch (P1, P3) with the symmetry related K1 ions.

The chains are decorated with $[Cu(bpca)]^+$ groups, where the Cu(II) cation features a slightly distorted square pyramidal geometry formed by the three nitrogen atoms of $bpca^-$ and by the O43 and O61 oxygen atoms of the P4 and P6 phosphate groups of two phytate anions, O43 residing in the apical position.

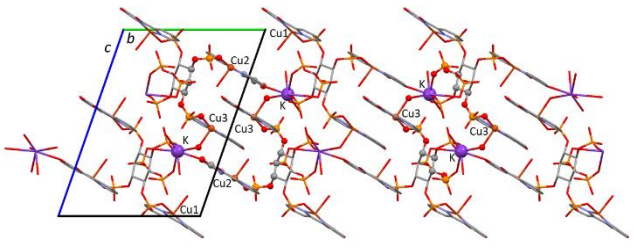

Figure 6. The 1D $(K(H_2O)_3\{[Cu(H_2O)(bpca)]_3H_8L\})_n$ polymeric coordination chains in **2** growing along the *b* crystallographic axis (light green arrow). Ball and stick graph is used to evidence the 32-membered and the 24-membered rings. H atoms and co-crystallized water molecules were omitted.

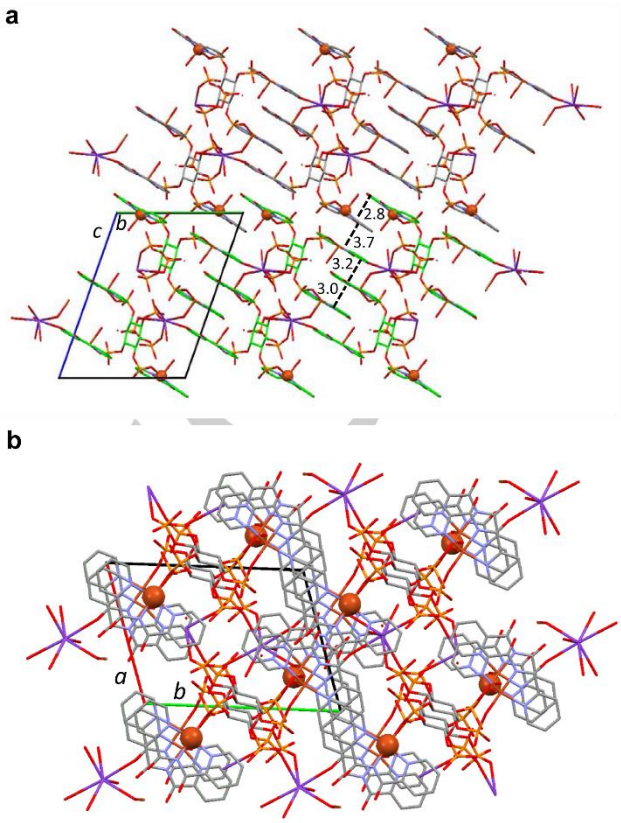

Figure 7. The crystal packing of **2**. 1D polymeric coordination chains viewed along the *a* (a) and *b* (b) crystallographic axes. Two parallel chains, depicting the formation of the 2D supramolecular assembly, are shown. In (a), carbon atoms are coloured green and grey, respectively, to highlight the two chains. Ball and stick graphs are used for Cu1. Distances are in Å.

As clearly shown in Figures 9b and 10, the additional K^+ ion is perfectly inserted into the 20-membered rings, where it is 10-coordinated by six phosphate oxygen atoms and four water molecules, with almost no modification of the structural motif of the 1D polymeric chain already observed in $K(H_2tptz)_{0.5}[Cu(tptz)(H_8L)]\cdot 3.6H_2O$ (see Figure 4b for comparison).

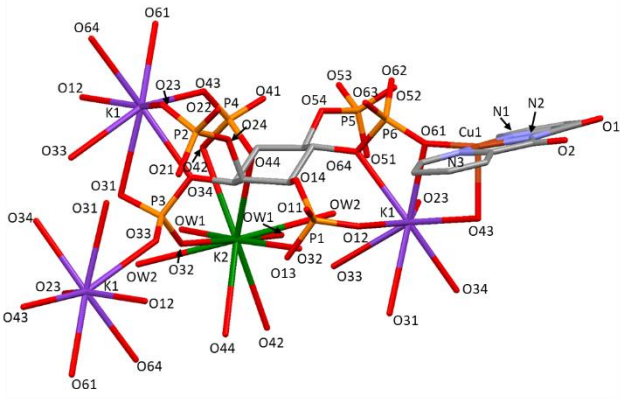

Figure 8. The basic structural unit in **3** with labelling scheme (H atoms omitted). Color code: C, grey, O, red, N, light blue, P, orange, K, violet and green, Cu, brown.

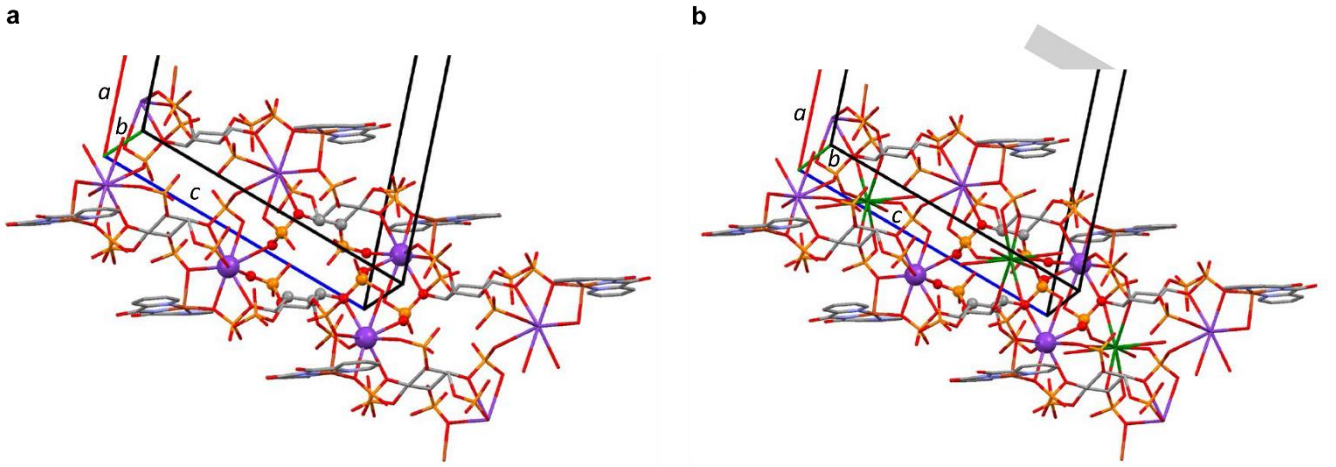

Figure 9. The 1D $\{K_{1.5}(H_2O)_2[Cu(bpca)](H_{9.5}L)\}_n$ coordination polymeric chain in **3**, growing along the *c* crystallographic axis (light green arrow) without (a) and with (b) the K2 ions (green coloured) into the 20-membered rings. Ball and stick graphs are used to evidence the 20-membered and the 8-membered rings.

Indeed, the structural motifs given by the 20-membered and 8-membered rings in the two structures (with and without the K^+ ion) can be finely superimposed (Figure S3, calculated RMSD of 0.14 Å), evidencing the high preorganization of the 20-membered ring to host the K^+ ion. Therefore, the overall packings of the two crystals appear to be influenced by the structural features of tptz and $bpca^-$ (Figure 11).

Co-crystallized water molecules form an H-bond network contributing to the overall stability of the crystal packing. Nevertheless, these water molecules are significantly disordered and, accordingly, their contacts are not further discussed.

Charge neutrality in this complex requires a fractional protonation degree of the phytate ligand ($H_{9.5}L^{2.5-}$) that we ascribe to the presence of equal amounts of nona- (H_9L^{3-}) and deca-protonated ($H_{10}L^{2-}$). Actually, the O23···O51 separation between symmetry related phytate anions (2.452(7) Å) agrees with the presence of a bridging acidic proton.

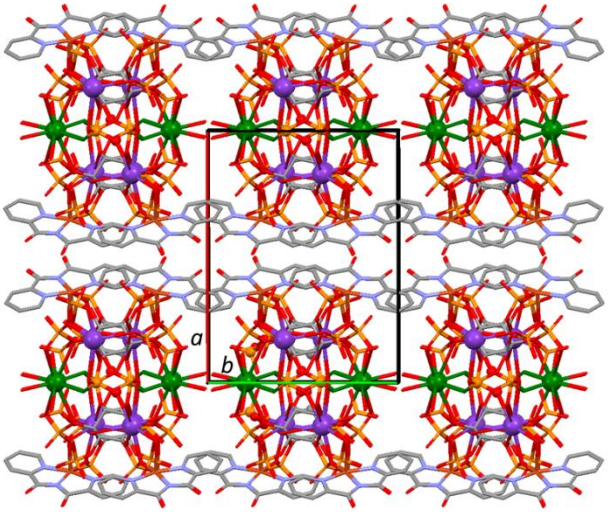

Figure 10. The crystal packing of **3** viewed along the *c* axis. K2 ions coloured in green; H atoms and cocrystallized water molecules omitted for clarity.

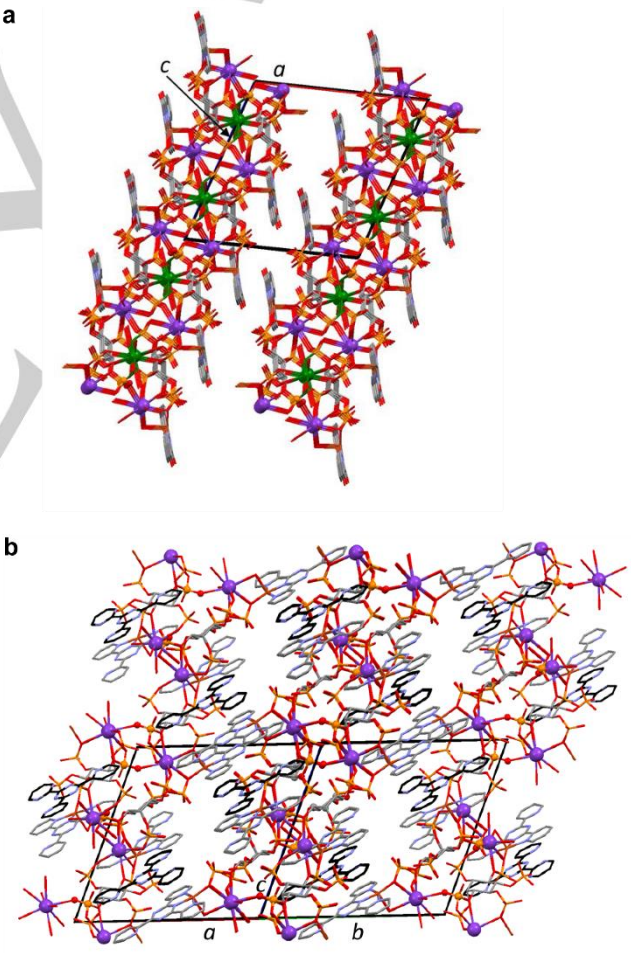

Figure 11. The crystal packing of **3** (a) viewed along the [0 1 0] direction (K2 ions coloured in green) and (b) viewed along the [1 1 0] direction. The direction of the crystallographic *c* axis is indicated with a light green arrow; H atoms and co-crystallized water molecules omitted.

Solution studies

The in solution studies included the determination of the acid-base constants of Hbpca, the complexation of Cu(II) with Hbpca, the hydrolysis constants of Cu(II) using the same metal ion concentration interval, the complexation of Cu(II) with Hbpca, the InsP_6–Hbpca interaction and the measure of the stability constants of the ternary system InsP_6–Cu–Hbpca. Table 1 shows the obtained results, which are in line with previous reports on similar systems.[36]

Bpca has three protonation steps corresponding to the amine and the two pyridyl groups. The deprotonated form $bpca^-$ gives rise to the neutral form Hbpca below pH 5.53, whereas the pyridyl groups are protonated only at more acidic pH (below pH 2.83 and 1.85, respectively). The potentially tridentate ligand $bpca^-$ forms stable complexes with copper(II) mostly in the deprotonated form. The complex species detected are: $[Cu(bpca)]^+$, $[Cu(bpca)_2]$, $[Cu(bpca)(Hbpca)]^+$ and [Cu(bpca)(OH)]. These complexes are similar to those reported for terpy under the same conditions[22c] even though the interaction in the case of Hbpca is slightly weaker than in the case of the less flexible amine terpy.

Hbpca interacts with phytate forming stable InsP_6:Hbpca 1:1 species with different protonation degree, a fact already observed for other heterocyclic polyamines[22b, 22c]. Species formed with the neutral or more protonated forms of Hbpca (according to the relative basicities of the interacting species) are formed in higher extent (see Figure S4 for [InsP_6] = [Hbpca] = 1 mM).

Finally, in the presence of copper(II), Hbpca and phytate, ternary species are also formed in line with previous reports using other amines[22b, 22c]. Figure 12 shows the distribution species diagram under the conditions of a typical potentiometric experiment ($[Cu^{2+}]$ = [Hbpca] = [InsP_6] = 1 mM). Protonated adducts with a 1:1:1 molar ratio are the predominant species formed in solution under these conditions. On the other hand, under conditions of InsP_6 defect, the polymeric species containing more than one $[Cu(bpca)]^+$ unit per InsP_6 become more abundant. This is shown in Figure S5 for $[Cu^{2+}]$ = [Hbpca] = 3 mM, [InsP_6] = 1 mM. A similar study for the system containing tptz was not possible due to the quick transformation to Hbpca in presence of Cu(II) (Figure 1c).

Cu(II)-assisted hydrolysis

Even though tptz hydrolysis requires vigorous conditions,[37] the process is efficiently catalyzed by Cu^{2+} ions (Figure 1c).[31, 38] This conclusion was stated after isolating, for the first time, a Cu(II) complex containing $bpca^-$ ($[Cu(bpca)(H_2O)_3]NO_3{\cdot}2H_2O$) from a tptz-Cu(II) aqueous solution. From that point onwards, several works have been reported concerning the structural elucidation of the hydrolytic mechanism, through the characterization of copper complexes containing tptz and some of its hydrolytic products.[31, 33b, 34-35, 38-39] A discussion of some of the most relevant results is included in the supporting information (Table S1).

Until now, the mechanism for the hydrolysis of tptz is not completely understood. Only one report has so far dealt with the

Table 1. Logarithms of the equilibrium constants for the reactions determined in this work (0.15 M NMe_4Cl at 37.0 °C).[a]

System	Equilibrium	log*K*
$bpca^-$ protonation	$bpca^- + H^+ = Hbpca$	5.53(3)
	$bpca^- + 2\,H^+ = H_2bpca^+$	8.21(4)
	$bpca^- + 3\,H^+ = H_3bpca^{2+}$	10.06(6)
Cu^{2+} hydrolysis	$Cu^{2+} + H_2O = [Cu(OH)]^+ + H^+$	–6.44(7)
	$Cu^{2+} + 2H_2O = [Cu(OH)_2] + 2H^+$	–12.7(6)
Cu^{2+}-$bpca^-$	$Cu^{2+} + bpca^- = [Cu(bpca)]^+$	7.35(7)
	$Cu^{2+} + 2bpca^- = [Cu(bpca)_2]$	12.1(1)
	$Cu^{2+} + Hbpca + bpca^- = [Cu(bpca)(Hbpca)]^+$	12.7(2)
	$Cu^{2+} + bpca^- + H_2O = [Cu(bpca)(OH)] + H^+$	0.37(6)
InsP_6-Hbpca	$L^{12-} + Hbpca + 3H^+ = [(bpca)(H_4L)]^{9-}$	37.4(1)
	$L^{12-} + Hbpca + 4H^+ = [(bpca)(H_5L)]^{8-}$	45.30(9)
	$L^{12-} + Hbpca + 5H^+ = [(bpca)(H_6L)]^{7-}$	51.6(1)
	$L^{12-} + Hbpca + 6H^+ = [(Hbpca)(H_6L)]^{6-}$	57.0(1)
	$L^{12-} + Hbpca + 7H^+ = [(Hbpca)(H_7L)]^{5-}$	61.2(1)
	$L^{12-} + Hbpca + 8H^+ = [(H_2bpca)(H_7L)]^{4-}$	63.8(2)
	$L^{12-} + Hbpca + 9H^+ = [(H_3bpca)(H_7L)]^{3-}$	66.8(2)
InsP_6-Cu^{2+}-Hbpca	$L^{12-} + Cu^{2+} + Hbpca + 2H^+ = [Cu(bpca)(H_3L)]^{8-}$	38.7(2)
	$L^{12-} + Cu^{2+} + Hbpca + 3H^+ = [Cu(bpca)(H_4L)]^{7-}$	48.23(6)
	$L^{12-} + Cu^{2+} + Hbpca + 4H^+ = [Cu(bpca)(H_5L)]^{6-}$	55.52(6)
	$L^{12-} + Cu^{2+} + Hbpca + 5H^+ = [Cu(bpca)(H_6L)]^{5-}$	62.03(7)
	$L^{12-} + Cu^{2+} + Hbpca + 6H^+ = [Cu(bpca)(H_7L)]^{4-}$	67.86(8)
	$L^{12-} + Cu^{2+} + Hbpca + 7H^+ = [Cu(bpca)(H_8L)]^{3-}$	72.7(1)
	$L^{12-} + Cu^{2+} + Hbpca + 8H^+ = [Cu(bpca)(H_9L)]^{2-}$	75.7(1)
	$L^{12-} + 2Cu^{2+} + Hbpca + 3H^+ = [Cu_2(bpca)(H_4L)]^{5-}$	56.41(8)
	$L^{12-} + 2Cu^{2+} + Hbpca + 4H^+ = [Cu_2(bpca)(H_5L)]^{4-}$	62.1(1)
	$L^{12-} + 2Cu^{2+} + 2Hbpca + H^+ = [Cu_2(bpca)_2(H_3L)]^{7-}$	47.34(4)
	$L^{12-} + 3Cu^{2+} + 3Hbpca + 4H^+ = [Cu_3(bpca)_3(H_7L)]^{2-}$	78.3(1)

[a] Formulas of the formed species in the InsP_6-Hbpca system are written according to relative basicity of InsP_6 and Hbpca forms. For copper containing species, according to the results obtained in the solid state, Hbpca ligand was maintained in the anionic form ($bpca^-$). The scaled sum of square differences between predicted and experimental values is 1.5 ($bpca^-$ protonation), 0.7 (Cu^{2+} hydrolysis), 0.4 (Cu^{2+}-$bpca^-$), 0.5 (InsP_6-Hbpca) and 0.4 (InsP_6-Cu^{2+}-Hbpca). Values given in parentheses are the 1σ statistical uncertainties in the last digit of the constant.

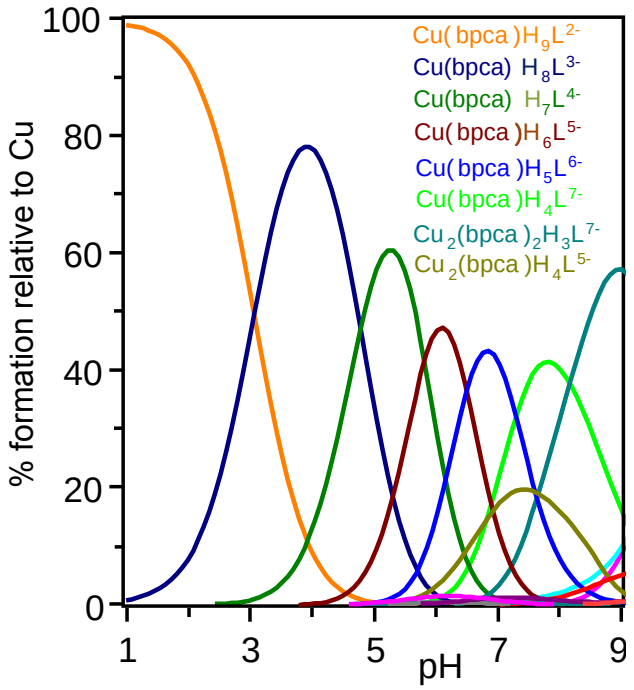

Figure 12. Species distribution diagram for Cu(II)-Hbpca-InsP_6 system, in 0.15 M NMe_4Cl at 37.0 °C. [Cu^{2+}] = [Hbpca] = [InsP_6] = 1 mM.

kinetic assessment of the reaction between the Cu(II)-tptz complex and water.[32a] In that work, Gillard and Williams followed the kinetic of the reaction recording the decrease of the absorbance of the solution at 410 nm. Nevertheless, only half of the entire hydrolytic process was characterized by determining a pseudo-first order rate constant for the nucleophilic attack on one of the electrophilic carbon atoms of the triazine ring (Figure S6). Moreover, the mechanistic proposal was based on the assumption that the first stage of the reaction involves a fast pre-equilibrium between the Cu(II)-tptz complex and its covalent hydrate species. This scenario is dubious; it entails that the nucleophilic attack by the water molecule is a low-activation energy process, although it destroys the aromaticity of the triazine ring. Nevertheless, a Rh(III)-tptz complex $[Rh(tptz)Cl_3]\cdot 2H_2O$ can be synthesized in high yield (85%) after refluxing in ethanol, and the two water molecules do not react; they remain nearby interacting with the electrophilic carbon atoms of the triazine ring by a through-space electrostatic forces.[32b]

In this context, we set out to kinetically reanalyze this system by monitoring the change in the visible spectra of a 10 mM Cu(II)-tptz aqueous solution as the reaction occurs at room temperature. The results, summarized in Figure S7a, show a hypsochromic shift in the copper *d-d* band with time, accounting for the observed green-to-blue color change of the solution. The kinetic fitting of the spectroscopic data indicated that more than one elementary step was taking place in the system, and the chemical model that best adjusted the experimental evidence led us to propose the mechanism depicted in Figure 13.

The first stage (A → B) would involve the nucleophilic attack of one water molecule on one of the carbon atoms adjacent to the metal-bound nitrogen atom (C_A or C_B), with a kinetic constant of k_1 = (3.23 ± 0.02) x 10^{-2} min^{-1}. Then, a fast tautomeric equilibria (K = 9.9) would be established between B and C. Finally, a second nucleophilic attack at the other carbon atom adjacent to the metal-bound nitrogen atom of the already opened triazine ring would be performed by another water molecule (C → D; k_4 = (2.825 ± 0.009) x 10^{-3} min^{-1}). Interestingly, the value of the pseudo-first order rate constant reported by Gillard and Williams (6.54 x 10^{-3} min^{-1} at 299 K) is intermediate between k_1 and k_4.[32a] In order to gather further evidence to support our mechanistic proposal, we DFT-optimized the geometry and modelled the electronic spectra of the involved species (A to D). The results are shown in Figures 13 and S7b. For D, only a Cu:Hbpca 1:1 complex was taken into account, based on the fact that it is the most abundant Cu(II)-bpca species under the conditions employed during the spectroscopic runs ([Cu] = [Hbpca] = 10 mM, pH = 6, see Figure S8 calculated from potentiometric results). For the other complexes A-C, a 1:1 Cu:ligand stoichiometry was also used as initial input for calculations. The individual calculated electronic spectra are in line with those experimentally determined, nicely reproducing the observed hypsochromic shift in the *d-d* band. It is worth noticing that this shift is mainly associated with the last step (C → D), for which a square pyramidal–trigonal bipyramidal transition is predicted to occur (see the τ values in Figure 13). Apart from the variation in the electron density brought about by the tptz-$bpca^-$ conversion, this structural phenomenon also seems to contribute to the observed green-to-blue color change between the tptz and $bpca^-$ Cu(II) soluble complexes. The role of the metal ion on the hydrolytic mechanism has been widely debated. At first, it had been suggested that the metal-induced angular strain was the main cause of the promotion of the tptz hydrolysis.[31, 38] In fact, the DFT-calculated angle values for β_A and β_B in $[Cu(H_2O)_2(tptz)]^{2+}$ are around 114°, showing a large offset from the ideal angle of 119° exhibited by free tptz (Table 2). Moreover, the complex $[Cu(bpca)(tptz)]CF_3SO_3$ (Table S1, entry 8) is not further hydrolyzed, in line with the fact that the crystallographic data show no angular strain. Nevertheless, 20 years ago Paul and co-workers found that the hydrolysis of tptz is not observed in the presence of Ru(II), even though angular strain occurred.[32b, 32c] Therefore, an electron-withdrawing effect of metal ions was proposed to promote tptz hydrolysis upon complexation and it was verified by NMR, structural and computational data.[32b, 32c, 40] Our computational results (Table 2) are also in agreement with this conclusion: when complexed with Cu^{2+}, the atomic charges of the electrophilic carbon atoms of tptz (C_A and C_B) increase from 0.45 to 0.50. In addition, the electrostatic potential near both atoms is significantly raised in the presence of the metal ion (compare Figures S9a and b). It is interesting to notice that previous DFT computational data on tptz and $[Cu(tptz)]^{2+}$ at similar level of theory also found a decrease in the N-C_A and N-C_B bond orders upon metal complexation.[40] On the contrary, our results suggest a slight reinforce of those bonds (Table 2). The difference may arise in the methodology to compute the bond orders: while in the previous report Mayer bond indexes were used (which do not provide approximately consistent results across different

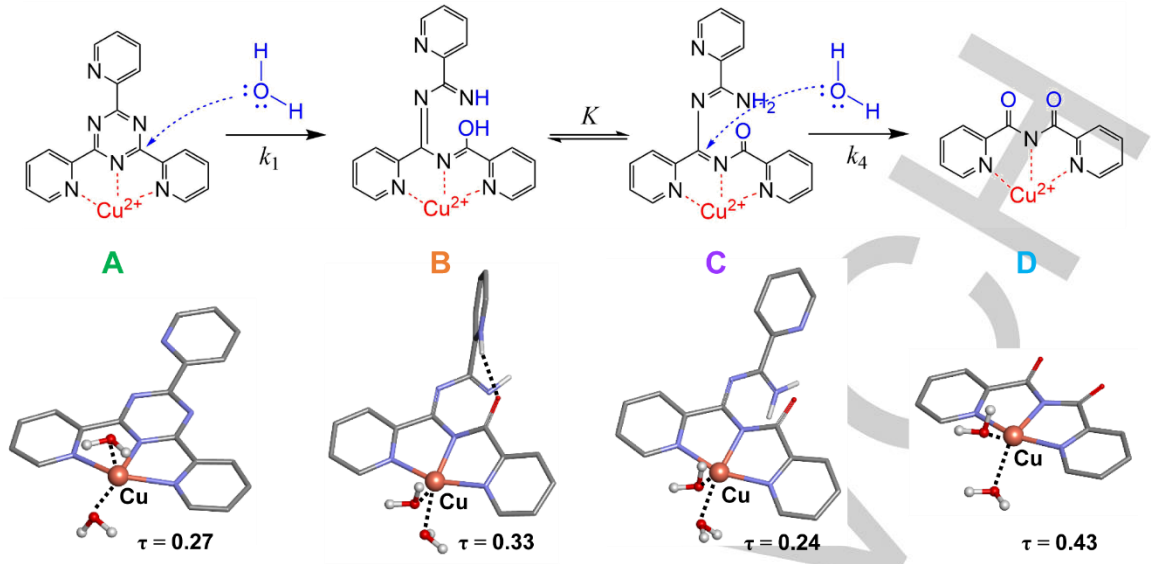

Figure 13. Proposed mechanism for the Cu(II)-mediated hydrolysis of tptz. The DFT optimized structures of the involved species (A – D) at UB3LYP/GEN – SMD level of theory and their geometry index (τ) are also shown. Atom color code: C (grey), H (white), O (red), N (blue), Cu (pink). Non-polar hydrogen atoms are omitted for clarity.

quantum chemistry methods), we employed the recently described and robust DDEC6 bond indexes.[41]

Lastly, to assess the influence of the phytate anion on the hydrolysis of tptz, we computationally determined some structural and electronic features of the complex $[Cu(H_8L)(H_2O)(tptz)]^{2-}$ (Table 2). Neither the atomic charges of C_A and C_B nor the angle values for β_A and β_B differ significantly from those determined for $[Cu(H_2O)_2(tptz)]^{2+}$. Indeed, when the hydrolytic reaction is kinetically analyzed in the presence of equimolar amounts of Cu^{2+} and phytate, and assuming the same mechanistic pathway depicted in Figure 13, the rate of tptz hydrolysis is only slightly increased: $k_1 = (3.89 \pm 0.03) \times 10^{-2}$ min^{-1}; $K = 8$; $k_4 = (3.92 \pm 0.02) \times 10^{-3}$ min^{-1}. Nonetheless, according to the uncertainty values this effect is statistically significant. A possible explanation for this trend could be the exceptionally large hydrated radius of the phytate anionic moiety,[16b, 42] which substantially concentrate the negative charge in the Cu(II)-tptz-phytate species (see Figure S9c). It is likely that some of those hydration water molecules can be activated, increasing their nucleophilicity through the formation of hydrogen bonds with the coordinated phytate anion. What is more, the presence of a small quantity of hydroxide anions surrounding the phytate species that can promote tptz alkaline hydrolysis cannot be ruled out.

Table 2. DFT structural and electronic parameters for tptz and its Cu(II) complexes.[a]

	tptz	$[Cu(H_2O)_2(tptz)]^{2+}$	$[Cu(H_8L)(H_2O)(tptz)]^{2-}$
Structural parameters			
β_A (°)	118.5	114.1	114.2
β_B (°)	118.8	114.3	114.4
N-C_A (Å)	1.34	1.33	1.33
N-C_B (Å)	1.34	1.33	1.33
Bond order			
N-C_A	1.37	1.41	1.41
N-C_B	1.36	1.41	1.41
Atomic charge			
C_A	0.45	0.50	0.49
C_B	0.44	0.50	0.50

[a] B3LYP/GEN – SMD optimized geometries (see experimental section).

Self-assembling processes

The gathered thermodynamic data can be used to reveal the most abundant species under the conditions employed to synthesize compound **2** (see the distribution diagram in Figure 14). In order to gain structural insights into the self-assembling processes that lead to the formation of **2**, we have also computationally determined their optimum geometry at a DFT level (Figure 14). For pH values between 2 and 3, the anionic species $[Cu(bpca)(H_9L)]^{2-}$ is predicted to interact with the cationic complex $[Cu(bpca)]^{+}$, giving rise upon deprotonation to the trinuclear complex $[Cu_3(bpca)_3(H_7L)]^{2-}$. Finally, the crystallization of **2** can be achieved when the negative charge of $[Cu_3(bpca)_3(H_7L)]^{2-}$ is neutralized by gaining one H^+ and one K^+ cations. It is worth noticing that, although different pH values were tried, the isolation of **2** could only be accomplished in the pH interval 2 – 3. For pH values below that range, the $bpca^-$ anion is substantially protonated, so the concentration of

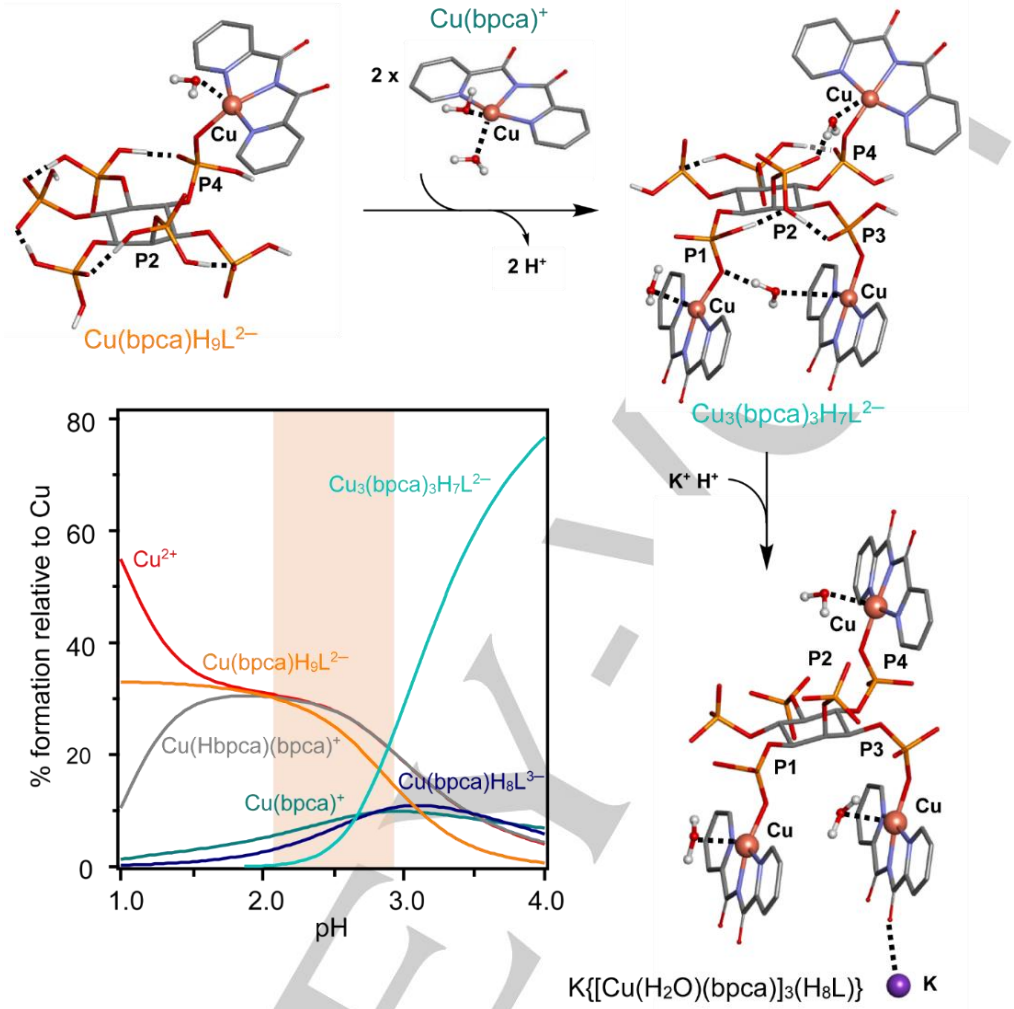

Figure 14. A possible mechanism for the self-assembling of Cu(II)-phytate-Hbpca soluble species to form **2**. Brackets are omitted for clarity. All involved species are formed in solution under the experimental conditions adopted to synthesize the complex according to the distribution diagram ([Hbpca] = [Cu(II)] = 30 mM; [phytate] = 10 mM). Structures are geometry optimized at UB3LYP/LANL2DZ – SMD level of theory. Atom color code: C (grey), H (white), O (red), N (blue), P (orange), Cu (pink). Non-polar hydrogen atoms are omitted for clarity. Polar hydrogen atoms are depicted only for the water molecules and the DFT-optimized phytate anions.

$[Cu(bpca)]^+$ is too low. Above pH 3, the H^+ concentration is not high enough to promote the neutralization of the $[Cu_3(bpca)_3(H_7L)]^{2-}$ species.

Self-assembling of **3** would probably follow a similar pathway, as it is obtained under synthetic conditions were the synthon $[Cu(bpca)]^+$ exist in moderate concentration.

Conclusions

The phytate anions are widely present in nature and play important biological roles. We have shown that they can be used as efficient building blocks for the assembling of extended structures in the presence of metal ions. This can be achieved when their polydentate character is coupled with the multiple interaction properties of aromatic polyamines with large delocalized π systems. Coordinative forces and supramolecular interactions, especially π-π stacking, were shown to hierarchically participate in the formation of 2D polymeric assemblies. Phytate forms the load-bearing 1D polymeric elements of the constructions via coordinative bridging interactions with several metal ions (K^+, Cu^{2+}), while the auxiliary tptz and $bpca^-$ ligands act as the π-π stacking glue sticking together these elements to form the 2D structures. Interestingly, the self-assembling of these compounds can be rationalized based on the equilibrium species formed, under thermodynamic control, in the solutions generating them. Furthermore, the rigidity of the auxiliary ligands favours the formation of highly preorganized constructions, as shown by the similar structural elements generated by tptz and $bpca^-$ in **1** and **3**, respectively, where a K^+ ion can be hosted with almost unappreciable structural modifications.

From this point of view, the properties of phytate recall those of lower-generation dendrimers,[43] opening up to possible applications in the creation of new families of nanostructured

functional materials. Accordingly, the solid-state properties of this molecule, which have remained unknown for a long time, suddenly appear to be manageable and hopefully useful for the development of material science and nanotechnology.

Experimental Section

Experimental Details The chemicals used throughout this work were purchased from commercial sources and used without further purification. $Cu(CO_2CH_3)_2$ (Aldrich, >99%), $CuCO_3$ (Aldrich, >98%) and $Cu_6(InsP_6)\cdot 14H_2O$[22c] were used as metal sources for the syntheses. The phytate dipotassium salt ($K_2H_{10}L\cdot 2.5\ H_2O$) was obtained from Sigma-Aldrich and the purity was rechecked by elemental and thermogravimetric analyses. 2,4,6-tris(2-pyridyl)-*s*-triazine (tptz) (>98%) was supplied by Sigma-Aldrich. Na_2EDTA (>99%) was purchased from Sigma-Aldrich. Methanol, $CHCl_3$, acetonitrile and acetone (99%) were obtained from Dorwill. Cu(II) solutions for the potentiometric titrations were prepared from $CuCl_2\cdot 2H_2O$ (Baker, >99%) and standardized according to standard techniques.[44] The ionic strength was adjusted to 0.15 M with NMe_4Cl (Fluka). The standard HCl solutions were prepared by diluting Merck standard ampoules. The titrant solution (0.1 M NMe_4OH in 0.15 M NMe_4Cl) was prepared by dissolving $NMe_4OH\cdot 5H_2O$ (Fluka) and was standardized with potassium biphthalate.

Infrared spectroscopy was carried out on a Shimadzu FT-IR spectrophotometer, with samples present as 1% KBr pellets. Elemental analysis (N, C, H) was performed on a Thermo Scientific FLASH 2000 CHNS/O instrument. Thermal analysis was performed on a Shimadzu TGA-50 instrument with a TA 50 I interface, using a platinum cell and nitrogen atmosphere. Experimental conditions were 0.5 °C min^{-1} temperature ramp rate and 50 mL min^{-1} nitrogen flow rate.

Syntheses

$K(H_2tptz)_{0.5}[Cu(H_8L)(tptz)]\cdot 9H_2O$ (**1**). 14.8 mg of $CuCO_3$ (0.12 mmol) was dissolved in 1 mL aqueous solution of $K_2H_{10}L\cdot 2.5H_2O$ (94 mg, 0.12 mmol). When the evolution of CO_2 ceased, 9 mL of water was added. Finally, 2 mL of a solution of tptz (75 mg, 0.24 mmol) in methanol was slowly added with stirring (pH = 2.0). After 12 weeks, dark green crystals of **1** (84 mg, 50%) were obtained upon liquid diffusion of acetone into this solution at room temperature, collected by filtration and air-dried. Found: N, 8.7; C, 28.0; H, 3.7%. Calc. for $C_{33}H_{51}N_9O_{33}P_6Cu_1K_1$: N, 9.1; C, 28.5; H, 3.7%. Thermal analysis agreed with the proposed formula: 11.1% weight loss corresponding to the elimination of water, compared with a calculated value of 11.7%. ν_{max}/cm^{-1} 3412 (O–H), 3080 and 2924 (C–H), 1578, 1541 and 1377 cm^{-1} (C=C, C=N), 1184–935 (O–P–O, PO–C); δ_{max}/cm^{-1} 503 (O–P–O); ρ_{max}/cm^{-1} 772 and 663 cm^{-1} (C–H, O-H). X-ray diffraction analysis of several crystals taken from different batches of compound **1** agreed to crystal structures corresponding to the formula $K(H_2tptz)_{0.5}[Cu(H_8L)(tptz)]\cdot 3.6H_2O$. Label (**1**) will be used to indicate both hydrated forms. A further discussion of infrared spectrum and thermal analysis is included in supporting information (Figures S10 – S15).

Hbpca. The Hbpca neutral form was synthesized by a modification of a previously reported procedure.[45] In detail, 290 mg of $Cu(CO_2CH_3)_2$ (1.6 mmol) and 500 mg of tptz (1.6 mmol) were dissolved in 50 mL of distilled water and a green solution was formed. This solution was heated at 70 °C until it turned blue and no further colour change occurred. When the aqueous solution reached room temperature, 1.8 g Na_2EDTA (4.8 mmol) and 50 mL of $CHCl_3$ were added for the ligand extraction. The mixture was stirred vigorously for two hours. The organic layer was separated, dried with anhydrous Na_2SO_4, and the free ligand was isolated in almost quantitative yield (331 mg, 91%) after removing the $CHCl_3$ by rotaevaporation. Found: N, 18.7; C, 63.3; H, 4.0%. Calc. for $C_{12}H_9N_3O_2$: N, 18.5; C, 63.4; H 4.0%. ν_{max}/cm^{-1} 1753 (C=O), 1483 cm^{-1} (C=C, C=N); ρ_{max}/cm^{-1} 746 and 617 cm^{-1} (C–H).

$K[Cu_3(bpca)_3(H_8L)]\cdot 10H_2O$ (**2**). 27 mg of Hbpca (0.12 mmol) was dissolved in 5 mL of methanol and added to a 10 mL aqueous solution containing $K_2H_{10}L\cdot 2.5H_2O$ (16 mg, 0.02 mmol) and $Cu_6(InsP_6)\cdot 14H_2O$ (26 mg, 0.02 mmol). The solution (pH ≈ 2.1 – 2.9) was poured into a screw cap test tube. Crystals of compound **2** (20.5 mg, 29%) were obtained after 24 weeks upon liquid diffusion of acetonitrile into this solution at room temperature. They were collected by filtration and air-dried. Found: N, 7.4; C, 30.3; H, 3.7%. Calc. for $C_{42}H_{58}N_9O_{40}P_6Cu_3K$: N, 7.2; C, 28.9; H 3.4%. Thermal analysis agreed with the proposed formula: 10.3% weight loss corresponding to the elimination of water, compared with a calculated value of 11.1%. ν_{max}/cm^{-1} 3422 (O–H), 3092 and 2932 (C–H), 1717 (C=O), 1636, 1605 and 1356 cm^{-1} (C=C, C=N), 1183–954 (O–P–O, PO–C); δ_{max}/cm^{-1} 490 (O–P–O); ρ_{max}/cm^{-1} 850, 760, 702 and 590 cm^{-1} (C–H, O-H). X-ray diffraction analysis of several crystals taken from different batches of compound **2** agreed to crystal structures corresponding to the formula $K(H_2O)_3\{[Cu(H_2O)(bpca)]_3(H_8L)\}\cdot 1.75H_2O$. Label (**2**) will be used to indicate both hydrated forms. A further discussion of infrared spectrum and thermal analysis is included in supporting information (Figures S10 – S15).

Compound **2** can also be obtained from tptz by means of the following procedure. 14.8 mg of $CuCO_3$ (0.12 mmol) was dissolved in 1 mL aqueous solution of $K_2H_{10}L\cdot 2.5H_2O$ (94 mg, 0.12 mmol). When the evolution of CO_2 ceased, 9 mL of water was added. Finally, 2 mL of a solution of tptz (37.5 mg, 0.12 mmol) in methanol was slowly added with stirring (pH = 2.6). After 16 weeks, blue crystals (34 mg, 49%) were obtained upon liquid diffusion of acetone into this solution at room temperature, collected by filtration and air-dried. Found: N, 7.6; C, 29.8; H, 3.9%. Calc. for $C_{42}H_{58}N_9O_{40}P_6Cu_3K$: N, 7.2; C, 28.9; H 3.4%.

$K_{1.5}[Cu(bpca)(H_{9.5}L)]\cdot 10H_2O$ (**3**). 14.8 mg of $CuCO_3$ (0.12 mmol) was dissolved in 1 mL aqueous solution of $K_2H_{10}L\cdot 2.5H_2O$ (32 mg, 0.04 mmol). When the evolution of CO_2 ceased, 9 mL of water was added. Finally, 2 mL of a solution of tptz (37.5 mg, 0.12 mmol) in methanol was slowly added with stirring (pH = 3.10). After 4 weeks, blue crystals (28 mg, 59%) were obtained upon liquid diffusion of acetonitrile into this solution at room temperature, collected by filtration and air-dried. Found: N, 4.0; C, 17.5; H, 3.5%. Calc. for $C_{42}H_{58}N_9O_{40}P_6Cu_3K$: N, 3.5; C, 18.2; H 3.7%. ν_{max}/cm^{-1} 3420 (O–H), 3092 and 2934 (C–H), 1717 (C=O), 1638, 1603 and 1364 cm^{-1} (C=C, C=N), 1190–937 (O–P–O, PO–C); δ_{max}/cm^{-1} 507 (O–P–O); ρ_{max}/cm^{-1} 760, 702, 652 and 631 cm^{-1} (C–H, O-H). X-ray diffraction analysis of several crystals taken from different batches of compound 3 agreed to crystal structures corresponding to the formula $K_{1.5}(H_2O)_2[Cu(bpca)](H_{9.5}L)\cdot 8H_2O$. Label (**3**) will be used to indicate both hydrated forms. A further discussion of infrared spectrum and thermal analysis is included in supporting information (Figures S10 – S15).

X-ray structure analysis

Crystals of $K(H_2tptz)_{0.5}[Cu(H_8L)(tptz)]\cdot 3.6H_2O$ (**1**, dark green), $K(H_2O)_3\{[Cu(H_2O)(bpca)]_3H_8L\}\cdot 1.75H_2O$ (**2**, blue) and $K_{1.5}(H_2O)_2[Cu(bpca)](H_{9.5}L)\cdot 8H_2O$ (**3**, blue) were used for X-ray diffraction analysis. A summary of the crystallographic data is reported in Table S2.

The integrated intensities were corrected for Lorentz and polarization effects and an empirical absorption correction was applied.[46] The structures were solved by direct methods.[47] Refinements were performed by means of full-matrix least-squares using SHELXL Version 2014/7.[48] All hydrogen atoms linked to carbon or nitrogen were introduced in calculated position and their coordinates were refined according to the linked atoms, with the exception of H25 and H26 in **1**, which were freely refined. Almost all water molecules were treated with partial occupancy factors. One phosphate group, in compounds **2** and **3**, respectively, was found spread over two positions and treated with partial occupancy factors: compound (**2**), 0.5 for O11, O13 and O11', O13'; compound **3**, 0.75 for O11, O12, O13 and 0.25 for O11', O12', O13'. In compound **1** the diprotonated tptz molecule is pseudosymmetric. As it lies on a 2-fold crystallographic axis passing through N9, C25, C28 and C29, carbon C27 and nitrogen N100 are related by symmetry and thus they were treated by using EXYZ and EADP instructions and 0.5 occupancy factors.

The CCDC number for **1**-**3**, 1884143-1884145, contains the supplementary crystallographic data for this paper. These data can be obtained free of charge from The Cambridge Crystallographic Data Centre via www.ccdc.cam.ac.uk/data_request/cif. Selected bond distances are reported in Tables S3–S5.

Hydrolysis studies

Tptz hydrolysis was studied by UV-vis spectroscopy at room temperature in 0.15 M NMe_4Cl aqueous solution. In a typical experiment, a solution containing tptz and Cu(II) (or tptz, Cu(II) and $K_2H_{10}L$) was prepared and the pH was adjusted to 6 with acetic/acetate buffer solution. Total concentrations of reactants were: tptz-Cu(II) system: [tptz] = [Cu] = 10 mM; tptz-Cu(II)-phytate system: [tptz] = [Cu] = [phytate] = 10 mM. Experimental conditions were chosen in order to maximize the absorbance values within the linear range. For each system, 100 spectra (400 – 800 nm) were recorded every 2.5 minutes on a UV-Vis Spectronic 2000 spectrophotometer, using 5 nm slit width and 1 cm optical path.

JPlus ReactLab Kinetics, a global kinetic analysis hard-modelling program was used to fit rate constant parameters and to calculate species absorbance spectra. The software minimizes the residual square sum (or ssq) which is a measure of the difference between the real data and that predicted by the current model and prevailing parameters. It does this by iteratively refining the free parameters of the model using an adaptation of a Marquardt-Levenberg algorithm and adjusting the 'colored' spectra, according to a least squares criterion.

Evolving Factor Analysis and Single Value Decomposition were used in the first instance to predict concentration profiles and spectra of ´colored´ components from the experimental data. It gives some indication of spectral shapes and the evolution of independent species during the measurement, which can offer useful insight into appropriate reaction models proposal for fitting.

Potentiometric measurements

The chemical behavior of InsP_6 in the presence of Hbpca and Cu(II) was analyzed through potentiometric titrations. The study was conducted according to our previous works,[22b, 22c] and the experimental concentration ranges used in the titrations are listed in Table S6. The equilibrium constants for phytate protonation and Cu(II)-InsP_6 complex formation measured under the same conditions were taken from our previous reports.[17a, 22c]

Overall equilibrium constants were adjusted to fit model predictions to experimental data by using the HYPERQUAD program.[49] Several chemically feasible stoichiometries were tried for each system (Hbpca protonation and complexation with Cu(II), InsP_6 interaction with Hbpca, and the formation of ternary species containing InsP_6, Hbpca and Cu(II)) and final models were selected on the basis of the σ parameter, the model confidence level estimator, chi-square, and the internal consistency of data reflected in standard deviations of the formation constants.[49] Species distribution diagrams were rendered with HySS.[50]

Computational calculations

The computational assessment of selected species in solution was performed in Gaussian 09[51] according to previous reports on similar systems.[22a, 22b] The initial geometries were built using the information given by the crystal structures of **1** and **2**, and the phytate protonation pattern was fixed according to the relative position of the ionisable groups. Water molecules were placed to complete the metal coordination sphere when needed. For the mononuclear species $[Cu(bpca)(H_9L)]^{2-}$, three different input structures where designed following the crystallographic evidence for compound **2**, in which the metal ion was coordinated by the phosphate groups at C1, C3 or C4. For the initial structural analysis, unrestricted Density Functional Theory (DFT) geometry optimization runs were carried out, using the B3LYP functional and the effective core potential LANL2DZ basis set.[52] The interaction with the bulk of the solvent was modeled through an IEFPCM method, with radii and non-electrostatic terms from Truhlar and coworkers' SMD solvation model.[53] All final structures were found to have only real vibrational frequencies. The outputs of the most stable structures were rendered with Discovery Studio Visualizer software.[54]

Further optimizations of the structures with a generic basis set (GEN) were performed to allow a better description of the electron density and molecular orbitals during the analysis of atomic charges, bond orders and electronic spectra. Geometry optimization was carried out using the B3LYP functional and the 6-31+G(d,p) basis set for C, H, N, O and P atoms.[55] Copper was treated using the effective core potential LANL2DZ relativistic procedure.[52] The Natural Population Analysis (NPA) phase of the Natural Bond Orbital analysis (NBO) was used to estimate the atomic charges.[56] As a quantitative measure of the bond order, the DDEC6 bond index[41] was calculated with the program Chargemol.[57] Excited state calculations using the time-dependent DFT method were carried out to model the electronic spectra. In each case, the first 50 singlet excited states were predicted at UB3LYP/6-311+G(d,p) level of theory.

Acknowledgements

The authors are grateful to CSIC (Programa de Apoyo a Grupos de Investigación, Uruguay) for financial support. The authors also thank Prof. Oscar Ventura and Prof. Kenneth Irving (Facultad de Química, Universidad de la República) for the access to the University computer cluster.

Keywords: chemical speciation • copper • potassium• phytate • X-ray diffraction

[1] V. Raboy, D. Bowen, *Subcell. Biochem.* **2006**, *39*, 71-101.
[2] S. Posternak, *Comptes Rendus de l'Academie des Sciences - Serie III* **1919**, *169*, 138-140.
[3] a) R. Irvine, *Biochemist* **2009**, *31*, 26-29; b) R. F. Irvine, M. J. Schell, *Nat. Rev. Mol. Cell Biol.* **2001**, *2*, 327-338; c) R. H. Michell, *Nat. Rev. Mol. Cell Biol.* **2008**, *9*, 151-161.

[4] a) B. S. Szwergold, R. A. Graham, T. R. Brown, *Biochem. Biophys. Res. Commun.* **1987**, *149*, 874-881; b) D. Pittet, W. Schlegel, D. P. Lew, A. Monod, G. W. Mayr, *J. Biol. Chem.* **1989**, *264*, 18489-18493.

[5] J. B. Martin, M. F. Foray, G. Klein, M. Satre, *BBA - Molecular Cell Research* **1987**, *931*, 16-25.

[6] a) S. B. Shears, *Subcell. Biochem.* **1996**, *26*, 187-226; b) O. Larsson, C. J. Barker, A. Sjoholm, H. Carlqvist, R. H. Michell, A. Bertorello, T. Nilsson, R. E. Honkanen, G. W. Mayr, J. Zwiller, P. O. Berggren, *Science* **1997**, *278*, 471-474.

[7] X. Zi, R. P. Singh, R. Agarwal, *Carcinogenesis* **2000**, *21*, 2225-2235.

[8] A. M. Efanov, S. V. Zaitsev, P. O. Berggren, *Proc. Natl. Acad. Sci. U. S. A.* **1997**, *94*, 4435-4439.

[9] H. Ji, K. Sandberg, A. J. Baukal, K. J. Catt, *J. Biol. Chem.* **1989**, *264*, 20185-20188.

[10] a) M. J. Berridge, R. F. Irvine, *Nature* **1989**, *341*, 197-205; b) F. S. Menniti, K. G. Oliver, J. Putney, S. B. Shears, *Trends Biochem. Sci.* **1993**, *18*, 53-56.

[11] J. D. York, A. R. Odom, R. Murphy, E. B. Ives, S. R. Wente, *Science* **1999**, *285*, 96-100.

[12] a) M. Yunmei, M. R. Lieber, *J. Biol. Chem.* **2002**, *277*, 10756-10759; b) M. R. Macbeth, H. L. Schubert, A. P. Vandemark, A. T. Lingam, C. P. Hill, B. L. Bass, *Science* **2005**, *309*, 1534-1539.

[13] E. Graf, J. W. Eaton, *Free Radic. Biol. Med.* **1990**, *8*, 61-69.

[14] A. Matejuk, A. Shamsuddin, *Curr. Cancer Ther. Rev.* **2010**, *6*, 1-12.

[15] W. N. Addison, M. D. McKee, *Bone* **2010**, *46*, 1100-1107.

[16] a) M. Ali, M. N. Shuja, M. Zahoor, I. Qadri, *Afr. J. Biotechnol.* **2010**, *9*, 1551-1554; b) S. B. Shears, *Cell. Signal.* **2001**, *13*, 151-158.

[17] a) J. Torres, S. Domínguez, M. F. Cerdá, G. Obal, A. Mederos, R. F. Irvine, A. Díaz, C. Kremer, *J. Inorg. Biochem.* **2005**, *99*, 828-840; b) J. Torres, N. Veiga, J. S. Gancheff, S. Domínguez, A. Mederos, M. Sundberg, A. Sánchez, J. Castiglioni, A. Díaz, C. Kremer, *J. Mol. Struct.* **2008**, *874*, 77-88; c) N. Veiga, J. Torres, S. Domínguez, A. Mederos, R. F. Irvine, A. Díaz, C. Kremer, *J. Inorg. Biochem.* **2006**, *100*, 1800-1810.

[18] a) N. Veiga, I. Macho, K. Gómez, G. González, C. Kremer, J. Torres, *J. Mol. Struct.* **2015**, *1098*, 55-65; b) N. Veiga, J. Torres, I. Macho, K. Gomez, G. Gonzalez, C. Kremer, *Dalton Trans.* **2014**, *43*, 16238-16251.

[19] G. E. Blank, J. Pletcher, M. Sax, *Acta Crystallogr.* **1975**, *B31*, 2584-2592.

[20] K. Cai, F. Sun, X. Liang, C. Liu, N. Zhao, X. Zou, G. Zhu, *Journal of Materials Chemistry A* **2017**, *5*, 12943-12950.

[21] M. Reinmuth, S. Pramanik, J. T. Douglas, V. W. Day, K. Bowman-James, *Eur. J. Inorg. Chem.* **2019**, 1870–1874.

[22] a) D. Quiñone, N. Veiga, J. Torres, C. Bazzicalupi, A. Bianchi, C. Kremer, *ChemPlusChem* **2017**, *82*, 721-731; b) D. Quiñone, N. Veiga, J. Torres, J. Castiglioni, C. Bazzicalupi, A. Bianchi, C. Kremer, *Dalton Trans* **2016**, *45*, 12156-12166; c) N. Veiga, J. Torres, C. Bazzicalupi, A. Bianchi, C. Kremer, *Chem. Commun.* **2014**, *50*, 14971-14974.

[23] F. H. Case, E. Koft, *J. Am. Chem. Soc.* **1959**, *81*, 905-906.

[24] B. Therrien, *J. Organomet. Chem.* **2011**, *696*, 637-651.

[25] D. A. Durham, G. H. Frost, F. A. Hart, *J. Inorg. Nucl. Chem.* **1969**, *31*, 571-574.

[26] a) L. Klepo, A. Copra-Janicijevic, L. Kukoc-Modun, *Molecules* **2016**, *21*, 101; b) J. Wei, N. Teshima, T. Sakai, *Anal. Sci.* **2008**, *24*, 371-376.

[27] Z. Kolarik, *Chem. Rev.* **2008**, *108*, 4208-4252.

[28] a) M. Salimi, K. Abdi, H. M. Kandelous, H. Hadadzadeh, K. Azadmanesh, A. Amanzadeh, H. Sanati, *BioMetals* **2015**, *28*, 267-278; b) J. Borrás, G. Alzuet, M. González- Alvarez, J. L. García- Giménez, B. Macías, M. Liu-González, *Eur. J. Inorg. Chem.* **2007**, *2007*, 822-834.

[29] R. Tabaraki, N. Sadeghinejad, A. Nateghi, *J. Fluoresc.* **2018**, *28*, 251-257.

[30] a) M. M. Najafpour, M. Hołyńska, A. N. Shamkhali, M. Amini, S. H. Kazemi, S. Zaynalpoor, R. Mohamadi, M. Bagherzadeh, T. Lis, *Polyhedron* **2012**, *34*, 202-209; b) B. Rezaei, M. Mokhtarianpour, A. A. Ensafi, H. Hadadzadeh, J. Shakeri, *Polyhedron* **2015**, *101*, 160-164.

[31] E. I. Lerner, S. J. Lippard, *J. Am. Chem. Soc.* **1976**, *98*, 5397-5398.

[32] a) R. D. Gillard, P. A. Williams, *Transition Met. Chem.* **1979**, *4*, 18-23; b) P. Paul, B. Tyagi, A. K. Bilakhiya, M. M. Bhadbhade, E. Suresh, G. Ramachandraiah, *Inorg. Chem.* **1998**, *37*, 5733-5742; c) P. Paul, B. Tyagi, M. M. Bhadbhade, E. Suresh, *J. Chem. Soc., Dalton Trans.* **1997**, *0*, 2273-2278.

[33] a) A. Kamiyama, T. Noguchi, T. Kajiwara, T. Ito, *Inorg. Chem.* **2002**, *41*, 507-512; b) T. Kajiwara, A. Kamiyama, T. Ito, *Chem. Commun.* **2002**, *0*, 1256-1257; c) A. Kamiyama, T. Noguchi, T. Kajiwara, T. Ito, *Angew. Chem. Int. Ed.* **2000**, *39*, 3130-3132.

[34] A. Cantarero, J. M. Amigo, J. Faus, M. Julve, T. Debaerdemaeker, *J. Chem. Soc., Dalton Trans.* **1988**, *0*, 2033-2039.

[35] Y.-Q. Zheng, W. Xu, F. Lin, G.-S. Fang, *J. Coord. Chem.* **2006**, *59*, 1825-1834.

[36] 5.83 ed., Academic Software, Sourby Old Farm, Timble, Otley, Yorks, LS21 2PW, UK, **2013**.

[37] E. M. Smolin, L. Rapoport, *S-Triazines and Derivatives*, Interscience Publishers, **1959**.

[38] E. I. Lerner, S. J. Lippard, *Inorg. Chem.* **1977**, *16*, 1546-1551.

[39] a) I. Castro, J. Faus, M. Julve, J. M. Amigo, J. Sletten, T. Debaerdemaeker, *J. Chem. Soc., Dalton Trans.* **1990**, *0*, 891-897; b) J. Faus, M. Julve, J. M. Amigo, T. Debaerdemaeker, *J. Chem. Soc., Dalton Trans.* **1989**, *0*, 1681-1687; c) K. Abdi, H. Hadadzadeh, M. Salimi, J. Simpson, A. D. Khalaji, *Polyhedron* **2012**, *44*, 101-112; d) Q. H. Zhao, M. S. Zhang, R. B. Fang, *J. Struct. Chem.* **2006**, *47*, 764-767; e) J. Borrás, G. Alzuet, M. González-Álvarez, F. Estevan, B. Macías, M. Liu-González, A. Castiñeiras, *Polyhedron* **2007**, *26*, 5009-5015; f) K. Abdi, H. Hadadzadeh, M. Weil, H. A. Rudbari, *Inorg. Chim. Acta* **2014**, *416*, 109-121.

[40] X.-P. Zhou, D. Li, S.-L. Zheng, X. Zhang, T. Wu, *Inorg. Chem.* **2006**, *45*, 7119-7125.

[41] T. A. Manz, *RSC Adv.* **2017**, *7*, 45552-45581.

[42] F. Irigoín, F. Ferreira, C. Fernández, R. B. Sim, A. Díaz, *Biochem. J.* **2002**, *362*, 297-304.

[43] a) M. Garzoni, N. Cheval, A. Fahmi, A. Danani, G. M. Pavan, *J. Am. Chem. Soc.* **2012**, *134*, 3349-3357; b) C. Bazzicalupi, A. Bianchi, C. Giorgi, P. Gratteri, P. Mariani, B. Valtancoli, *Inorg. Chem.* **2013**, *52*, 2125-2137 and references therein cited.

[44] G. Schwarzenwach, H. Flaschka, *Complexometric Titrations*, 2nd ed., Methuen, London, **1969**.

[45] R. Sahu, S. K. Padhi, H. S. Jena, V. Manivannan, *Inorg. Chim. Acta* **2010**, *363*, 1448-1454.

[46] SADABS-2016/2, Bruker (2016/2) for $K(H_2tptz)_{0.5}[Cu(tptz)(H_8L)]\cdot 3.6H_2O$ (**1**); CrysAlisPro, Agilent Technologies, Version 1.171.35.11 for $K(H_2O)_3\{[Cu(H_2O)(bpca)]_3H_8L\}\cdot 1.75H_2O$ (**2**) and $K_{1.5}(H_2O)_2[Cu(bpca)](H_{9.5}L)\cdot 8H_2O$ (**3**).

[47] SHELXT 2014/5 - G. M. Sheldrick, *Acta Cryst. A*, 2015, **71**, 3-8 for (**1**); Olex - O.V. Dolomanov, L.J. Bourhis, R.J. Gildea, J.A.K. Howarda and H. Puschmanna, *J. Appl. Cryst.*, 2009, **42**, 339–341 for (**2**) and SIR92 - A. Altomare, G. Cascarano, C. Giacovazzo, A. Guagliardi, M.C. Burla, G. Polidori and M. Camalli, *J. Appl. Cryst.* 1994, **27**, 435 for (**3**).

[48] G. Sheldrick, *Acta Crystallogr., Sect. C: Cryst. Struct. Commun.* **2015**, *71*, 3-8.

[49] P. Gans, A. Sabatini, A. Vacca, *Talanta* **1996**, *43*, 1739-1753.

[50] L. Alderighi, P. Gans, A. Ienco, D. Peters, A. Sabatini, A. Vacca, *Coord. Chem. Rev.* **1999**, *184*, 311-318.

[51] M. J. Frisch, G. W. Trucks, H. B. Schlegel, G. E. Scuseria, M. A. Robb, J. R. Cheeseman, G. Scalmani, V. Barone, B. Mennucci, G. A. Petersson, H. Nakatsuji, M. Caricato, X. Li, H. P. Hratchian, A. F. Izmaylov, J. Bloino, G. Zheng, J. L. Sonnenberg, M. Hada, M. Ehara, K. Toyota, R. Fukuda, J. Hasegawa, M. Ishida, T. Nakajima, Y. Honda, O. Kitao, H. Nakai, T. Vreven, J. Montgomery, J. E. Peralta, F. Ogliaro, M. J. Bearpark, J. Heyd, E. N. Brothers, K. N. Kudin, V. N. Staroverov, R. Kobayashi, J. Normand, K. Raghavachari, A. P. Rendell, J. C. Burant, S. S. Iyengar, J. Tomasi, M. Cossi, N. Rega, N. J. Millam, M. Klene, J. E. Knox, J. B. Cross, V. Bakken, C. Adamo, J. Jaramillo, R. Gomperts, R. E. Stratmann, O. Yazyev, A. J. Austin, R. Cammi, C. Pomelli, J. W. Ochterski, R. L. Martin, K. Morokuma, V. G. Zakrzewski, G. A. Voth, P. Salvador, J. J. Dannenberg, S. Dapprich, A. D. Daniels, Ö. Farkas, J. B. Foresman, J. V. Ortiz, J. Cioslowski, D. J. Fox, Gaussian, Inc., Wallingford, CT, USA, **2009**.

[52] P. J. Hay, W. R. Wadt, *J. Chem. Phys.* **1985**, *82*, 299-310.

[53] A. V. Marenich, C. J. Cramer, D. G. Truhlar, *J. Phys. Chem. B* **2009**, *113*, 6378-6396.

[54] 2.5.5.9350 ed., Accelrys Software Inc., **2009**.

[55] R. Ditchfield, W. J. Hehre, J. A. Pople, *J. Chem. Phys.* **1971**, *54*, 724-728.

[56] a) J. P. Foster, F. Weinhold, *J. Am. Chem. Soc.* **1980**, *102*, 7211-7218; b) A. E. Reed, F. Weinhold, *J. Chem. Phys.* **1985**, *83*, 1736-1740; c) A. E. Reed, R. B. Weinstock, F. Weinhold, *J. Chem. Phys.* **1985**, *83*, 735-746.

[57] T. A. Manz, N. Gabaldon Limas, Version 3.5 ed., ddec.sourceforge.net, **2017**.

Entry for the Table of Contents

FULL PAPER

The naturally occurring phytate molecule, assisted by aromatic amines, forms polynuclear Cu^{2+} complexes in aqueous solution. In the solid state, coordinative forces and supramolecular interactions cooperate in the formation of 2D polymeric assemblies. Phytate forms the load-bearing 1D polymeric elements of the constructions via coordinative bridging interactions with several metal ions (K^+, Cu^{2+}), while the auxiliary aromatic ligands act as the π-π stacking glue sticking together these elements to form the 2D structures.

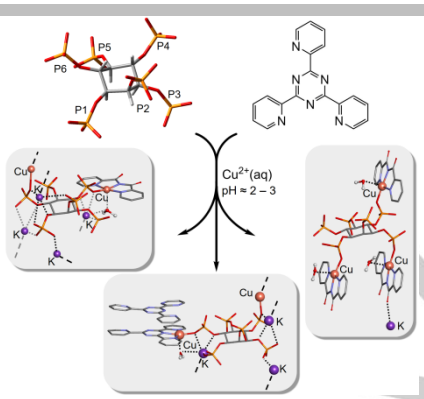

*Author(s), Corresponding Author(s)**

Page No. – Page No.

Title